Core-electron relaxation energies and valence-band formation of linear alkanes studied in the gas phase by means of electron spectroscopy

J. J. Pireaux,* S. Svensson, E. Basilier, P-Å Malmqvist, U. Gelius, R. Caudano,* and K. Siegbahn
Institute of Physics, Uppsala University, P.O. Box 530, S-751 21, Uppsala, Sweden
(Received 17 May 1976)

Core- and valence-electron spectra of the n-alkanes have been recorded under high resolution in the gas phase. The measured core-level binding energies decrease with an increasing number of carbon atoms in the molecules. The whole shift ranges over 0.6 eV. These small shifts are ruled by the relaxation energy and are discussed with the aid of various theoretical models. It is found that the transition-potential model together with CNDO/2 (complete neglect of differential overlap) calculations describes satisfactorily the variation of the core-level binding energies. The shakeup spectra of methane, ethane, and propane are presented and tentatively interpreted. The valence-electron structures of methane, ethane, propane, n-butane, and n-pentane are studied. Results are correlated with *ab initio* calculations using an extended basis set. The formation of a valence-electron band is discussed. For instance, it appears that n-tridecane provides a convenient finite model for the band structure of an infinite linear polymer.

I. INTRODUCTION

It is a general observation that core-electron binding energies for free atoms or molecules are larger than for the corresponding liquids or solids. The same is true also going from free atoms to their corresponding diatomic molecules. In all these cases the effect is due to the fact that the larger systems have available more degrees of freedom for electronic reorganization upon the ionization of a core orbital. This will increase the relaxation energy, which causes a corresponding decrease in electron binding energy. The n-alkanes C_nH_{2n+2} provide a suitable series of molecules for studying this effect since the molecular size can be increased stepwise and the compounds can be studied as free molecules even for quite large values of n.

When two identical atoms are brought together to form a molecule the electronic levels split. This splitting will be more pronounced for the outermost shells of the molecule, where the overlap between the orbitals is larger. Increasing the number of identical atoms (or groups of atoms) in the molecule implies a corresponding increase in the level density, and thus illustrates the formation of a band structure. The alkane series is also suitable for studying this effect. The successive molecules with an increasing n are considered as progressive steps in the construction of an ideal one-dimensional solid.

As a first step it is preferable to work with gases, thereby avoiding the disturbing influence of intermolecular interactions. Several gas-phase studies of the alkanes have appeared in the literature. However, electron spectra excited by x rays have been obtained only for the first members of the the series,[1,2] whereas uv-excited electron spectra[3-6] are handicapped by a very low photoionization cross section for s orbitals.[4,10] In the present study ESCA (electron spectroscopy for chemical analysis) spectra from methane to n-tridecane ($n = 1-13$) were obtained in the gas phase using monochromatized Al $K\alpha$ excitation. Corresponding spectra from the molecules $n = 5$ to ∞ have previously been recorded in the solid phase.[7-9]

II. EXPERIMENTAL PROCEDURE

All the samples were obtained commercially and used without further purification. Gases (methane to n-butane, research grade 99.95%) were obtained from Phillips Petroleum Co.; liquid samples (n-pentane to n-tridecane) of at least 99% purity were purchased from Aldrich Chemicals.

The spectra were recorded with an ESCA spectometer previously described.[11] Briefly it can be characterized by monochromatization of the exciting Al $K\alpha$ radiation in the fine-focusing scheme and by multichannel electron detection. The samples were studied at a typical pressure of 50 Pa. Lower pressures ($\lesssim 10$ Pa) were used to check the possible influence of electro inelastic scattering on the spectra. The core lines were calibrated by mixing the alkane with CO_2 and by recording simultaneously the two C 1s peaks (CO_2: C 1s = 297.69 eV[12]). The molecular-orbital region was similarly calibrated by mixing the gas with argon (Ar 3s = 29.23 eV and Ar 3p = 15.81 eV[12]).

TABLE I. Experimental binding energies of the C1s level of the alkanes (eV).

Compound	Binding energy [a] and chemical shift [b] Peak position [c]	Centroid [d]
CH_4	290.76	290.83
	0.0	0.0
C_2H_6	290.64	290.71
	−0.12	−0.12
C_3H_8	290.52	290.57
	−0.24	−0.26
n-C_4H_{10}	290.44	290.48
	−0.32	−0.35
n-C_5H_{12}	290.36	290.42
	−0.40	−0.41
n-C_6H_{14}	290.31	290.36
	−0.45	−0.47
n-C_8H_{18}	290.23	290.31
	−0.53	−0.52
n-$C_{10}H_{22}$	290.19	290.27
	−0.57	−0.56
n-$C_{13}H_{28}$	290.15	290.26
	−0.61	−0.57

Literature results

	Siegbahn (Ref. 1)	Thomas (Ref. 13)	Perry (Ref. 14)	Shirley (Ref. 15)
CH_4	290.7	290.8	290.74	290.7
C_2H_6		290.6	290.58	290.5
C_3H_8				290.5

[a] Calibrated with respect to CO_2 C 1s at 297.69 ± 0.14 eV.
[b] Chemical shift relative to CH_4 C1s line.
[c] Estimated error: ±0.04 eV.
[d] Estimated error: ±0.02 eV.

III. CORE LEVELS

A. Chemical shifts

The experimental alkane C 1s binding energies relative to the vacuum level are shown in Table I together with some previously published data. Two sets of values are given, peak positions and centroids. The centroids were calculated by computer fitting of Gaussians. Vibrational broadening of the core lines[16,17] causes asymmetry in the recorded peaks, resulting in a difference between peak and centroid positions. The vertical ionization energies are best deduced from the centroids.[18] The chemical shifts, included in Table I for convenience, are very small, less than 0.6 eV. Nevertheless, as the centroids have been determined to within ±0.02 eV, we are able to observe a very smooth variation of binding energies versus the number of carbon atoms in the molecules (Fig. 1).

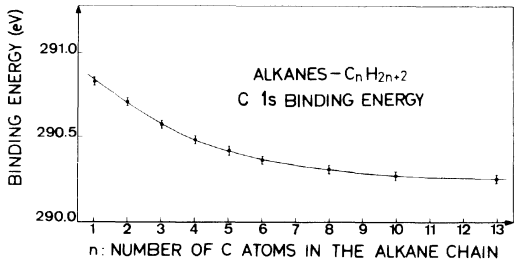

FIG. 1. Carbon 1s binding energies (centroid of the peak) of the alkanes: C_nH_{2n+2}.

B. Theoretical correlations

ESCA chemical shifts are understood[1,19] quite well and can be correlated with data from various models ranging from simple charge correlations to accurate *ab initio* calculations on ground and hole states. Below we will discuss the shifts of the alkanes in terms of some of these models. Since the measured energy range of the shifts in this series of molecules is very small one cannot *a priori* expect to find the normal trend of increasing binding energy with increasing positive charge on the atom considered. In fact, it is interesting to note that both simple electronegativity arguments and *ab initio* calculations predict an increasing average charge on the carbon atoms with increasing n, whereas the C1s binding energy decreases as seen from Fig. 1.

As a next step of refinement, the electrostatic interaction from the other atoms in the molecule can be accounted for in the ground-state potential model[1] (GPM):

$$\Delta E_A = k_A q_A + V_A + L, \tag{1}$$

The comparison between experimental shifts and values calculated by the potential model, using CNDO/2 (complete neglect of differential overlaps) charges and $k_A = 22.1$ eV/(unit charge), is shown in Fig. 2. The GPM does not significantly improve the simple charge correlation. Both the signs and

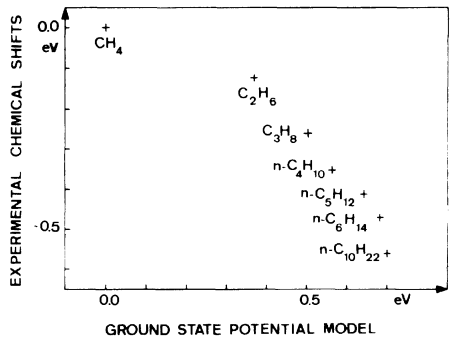

FIG. 2. Correlation between ESCA binding energies of the alkane C 1s peaks and the ground-state potential model (GPM).

TABLE II. CNDO/2 analysis of the alkanes: Populations and potentials in ground-state (G) and transition-potential (T) models, together with estimation of the relaxation energy for C 1s ionization.

Compound	P_A^G	P_A^T	ΔP_A	V_A^G (eV)	V_A^T (eV)	ΔV_A (eV)	ΔE_B [a] (eV)	E_R [b] (eV)	r_{eff} [d] (Å)
CH_4-C_1	4.050	4.549	0.500	0.654	7.240	6.586	0.0	14.1 [c]	1.09
C_2H_6-C_1	4.006	4.497	0.492	0.058	5.572	5.514	−0.40	14.9	1.28
C_3H_8-C_1	3.976	4.461	0.485	−0.269	4.450	4.719	−0.62	15.4	1.48
C_2	4.009	4.505	0.496	0.147	5.546	5.399		15.1	1.32
n-C_4H_{10}-C_1	3.978	4.469	0.491	−0.161	4.429	4.596	−0.82	15.7	1.54
C_2	4.010	4.507	0.497	0.143	5.431	5.288		15.2	1.35
n-C_5H_{12}-C_1	3.978	4.475	0.497	−0.058	4.407	4.465	−0.93	16.0	1.60
C_2	3.978	4.469	0.491	−0.146	4.341	4.487		15.8	1.57
C_3	4.005	4.504	0.499	0.078	5.298	5.220		15.4	1.38
n-C_6H_{14}-C_1	3.980	4.478	0.497	−0.029	4.371	4.400	−1.00	16.1	1.63
C_2	3.977	4.468	0.491	−0.167	4.286	4.453		15.9	1.58
C_3	4.004	4.504	0.499	0.060	5.259	5.199		15.4	1.38
n-$C_{10}H_{22}$-C_1	3.983	4.481	0.498	−0.040	4.228	4.268	−1.09	16.2	1.68
C_2	3.983	(4.47)	(0.487)	−0.042	(4.22)	(4.26)		16.0	1.64
C_3	3.980	(4.47)	(0.492)	−0.064	(4.279)	(4.343)		16.0	1.63
C_4	3.978	4.470	0.492	−0.187	4.233	4.420		15.9	1.60
C_5	4.004	(4.503)	(0.499)	0.045	(5.22)	(5.176)		15.4	1.38

[a] Binding energy [Eq. (3)]; C 1s shifts, referred to CH_4 C 1s line. The value is the arithmetic average over shifts on all the carbon atoms in the molecule.

[b] Relaxation energy according to Eq. (5) with methane as a reference.

[c] *Ab initio* result from Ref. 25.

[d] r_{eff} is the effective radius; see text for definition.

the trends of these calculated binding-energy shifts are incorrect. Treating k_A as an adjustable parameter leads to a least-squares value of 3.76 eV/(unit charge). Besides being unacceptably small from a theoretical point of view, this value also gives a very poor correlation.

As has previously been discussed,[20] the chemical shift is determined not only by the ground-state charge distribution. The final-state influence is generally accounted for as a relaxation term. In this picture the charge distribution is rearranged upon ionization. This can be described as two effects, namely, a contraction of the orbitals around the localized core hole and a flow of electron density to the corresponding atom:

$$E_R = E^{\text{contr}} + E^{\text{flow}} , \tag{2}$$

The contraction part is, to a first approximation, proportional to the charge on the atom before ionization.[20,21] The flow part can be accounted for in terms similar to those in the potential model [Eq. (1)], i.e., in terms of the amount of charge flow to the atom considered and a molecular potential from the other atoms caused by the charge redistribution. The first term is to be multiplied by an electrostatic integral for the core-valence elec-

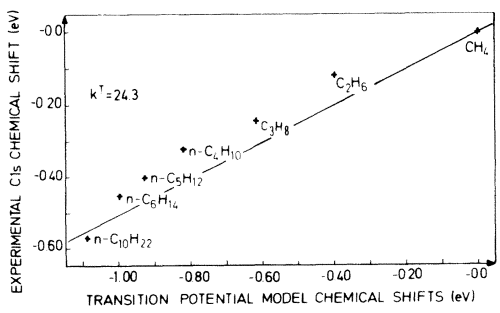

FIG. 3. Correlation between ESCA binding energies of the alkane C 1s lines and the transition-potential predictions.

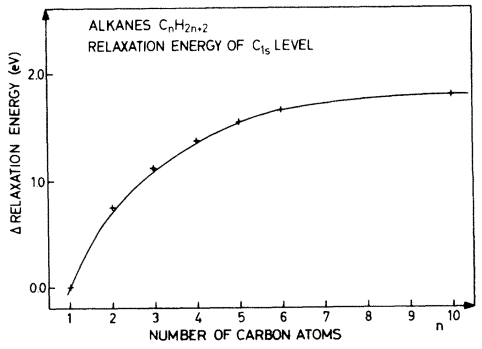

FIG. 4. Relaxation energy for the C 1s level of the alkanes, as calculated in the transition-potential model.

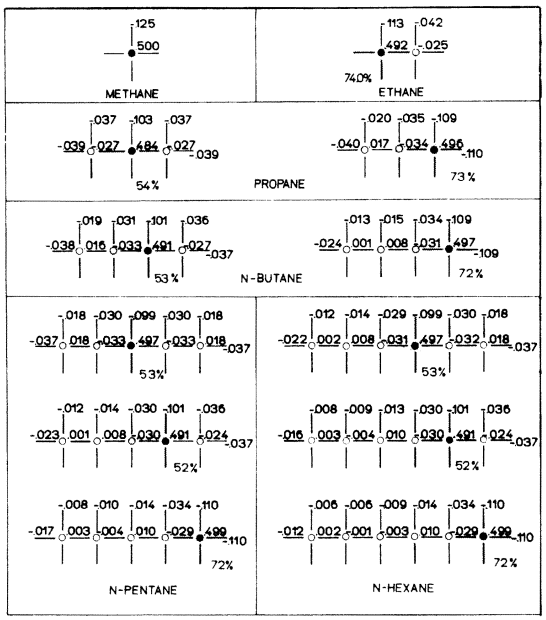

FIG. 5. Charge flow ΔQ (difference in charge before and after ionization of the atom marked by a black dot). The percentage value given under each molecule gives the amount of charge flow from the nearest neighbors (shaded area) relative to the total charge flow.

tron interaction.

The effects of relaxation are implicitly included in the transition-potential model[22,23] for ESCA shifts:

$$\Delta E_B = k_A^T q_A^T + V_A^T + L^T, \tag{3}$$

where the charge on atom A, q_A^T, and the molecular potential V_A^T are calculated for a transition state obtained for a transition operator,[24] which is an intermediate of the Fock operators of the ground and of the final states. The relaxation energy is given by[23] the difference between Eq. (1) and Eq. (3):

$$-E_R = (k_A^T - k_A)q_A + k_A^T(q_A^T - q_A) + (V_A^T - V_A) + L^T - L. \tag{4}$$

This is conveniently rewritten in terms of valence-electron populations P_A instead of charges:

$$E_R = (k_A^T - k_A)P_A + k_A^T(P_A^T - P_A) + V_A - V_A^T + C, \tag{5}$$

with

$$C = L - L^T - Z(k_A^T - k_A) - k^T(Z^T - Z). \tag{6}$$

Here, Z and Z^T stand for the nuclear charge minus the number of core electrons in the ground state and in the transition state, respectively. The first term in Eq. (5) is recognized as the contraction term E^{contr} in Eq. (2). The second and third terms

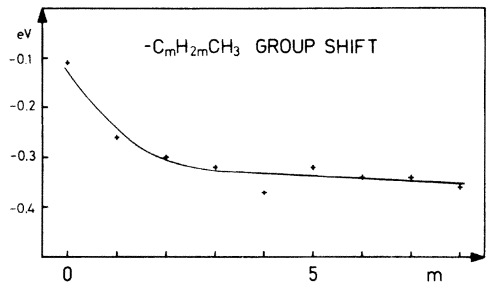

FIG. 6. Group-shift prediction for a $-C_mH_{2m}CH_3$ ($0 \le m \le n-2$) group. The group shift for $-$ H was taken to be 0.01 eV.

are the potential terms set up by the electron flow. The first of these will be called the screening potential and the second term will be called the molecular relaxation potential. It should be noticed that, with the above sign conventions, i.e., having a positive total relaxation energy, the molecular relaxation potential is always negative, so that it counteracts the screening potential. Using the CNDO/2 values $k_A^T = 24.3$ and $k_A = 22.1$ eV/(unit charge),[23] we can adjust $L - L^T$ to reproduce the methane relaxation energy 14.10 eV, which has been accurately determined by PNO-CI (pseudo-natural orbitals-configurations interactions) calculations.[25] In this way we obtain $C = -0.40$ eV for carbon atoms.

Table II reports the populations and molecular potentials deduced from CNDO/2 calculations. The atoms are labeled from the center of the molecule to one end. Figures between brackets were obtained by interpolation. The correlation between experimental shifts and values calculated using the transition-potential model is shown in Fig. 3. The scattering of the data from the fitted straight line is of the order of 0.1 eV, which is in the limit of

TABLE III. Carbon 1*s* binding energies (BE) of the alkanes (eV) by *ab initio* (extended basis STO-4.31G) calculations in the Koopmans approximation.

Molecule	C 1s BE (eV)	Average BE (eV)	C charge
methane	304.44	304.44	−0.6097
ethane C_1	304.67	304.67	−0.4478
C_2	304.67		−0.4478
propane C_1	304.71	304.54	−0.3120
C_2	304.46		−0.4393
C_3	304.46		−0.4393
n-butane C_1	304.76	304.68	−0.3002
C_2	304.59		−0.4416
C_3	304.76		−0.3002
C_4	304.59		−0.4416

TABLE IV. *Ab initio* (STO-3G) total energies and C1*s* chemical shifts of the alkanes in eV.

Molecule	Total energies: Ground state	Total energies: Hole state [a]	C1*s* chemical shifts: Koopmans' energies		C1*s* chemical shifts: ΔSCF energies	
methane	−1080.9578	−1519.9461	0.00		0.00	
ethane	−2130.6627	−2569.9738	0.14		−0.32	
propane C_1	−3180.4648	−3620.0778	0.32	0.14 [b]	−0.62	−0.60 [b]
C_2		−3620.0312	0.05		−0.58	
n-butane C_1	−4230.1690	−4669.9562	0.22	0.15 [b]	−0.80	−0.68 [b]
C_2		−4669.7099	0.08		−0.55	

[a] Equivalent-core approximation.
[b] Arithmetic average.

the model accuracy.[23,26,27] The slope of the line (0.5), however, is far from the unit slope obtained on other molecules.[22]

The C1*s* relaxation energies deduced from Eq. (5) are given in the ninth column in Table II and plotted also in Fig. 4. A comparison with Fig. 1 suggests that the relaxation energy is the major contribution to the C1*s* chemical shifts in the alkane series. A closer inspection of the terms involved in the expression for the relaxation energy shows that the variation in the relaxation energy throughout the alkane series is almost entirely given by the molecular relaxation potential. Thus, the contraction term and the screening potential are practically constant, actually both decreasing by 0.15 eV, whereas the total relaxation energy increases with increasing *n*. It is interesting to note that the screening, amounting to 0.50 electrons, is complete already for methane despite the fact that the carbon atom in this case is surrounded by hydrogens only. With increasing molecular size, the electron flow can be taken from more and more distant atoms and hence the counteracting molecular relaxation potential decreases, resulting in an increasing total relaxation. In order to illustrate this molecular size effect we have introduced an effective radius r_{eff}, defined by the molecular relaxation expression

$$\Delta V_A = V_A^T - V_A^G = (P_A^T - P_A^G)/r_{\text{eff}} . \tag{7}$$

r_{eff} is given in Table II, column 10, and is seen to increase with the size of the molecule to an asymptotic value which is only slightly larger than the C-C interatomic distance. The charge flow is also illustrated in Fig. 5. As can be seen all the atoms effectively participate in the screening of the core hole and the contribution from the first neighbors decreases with increasing size of the molecule. It is also interesting to note the alternating pattern of the charge flow for the carbon atoms.

Our results for *n*-hexane can be compared to

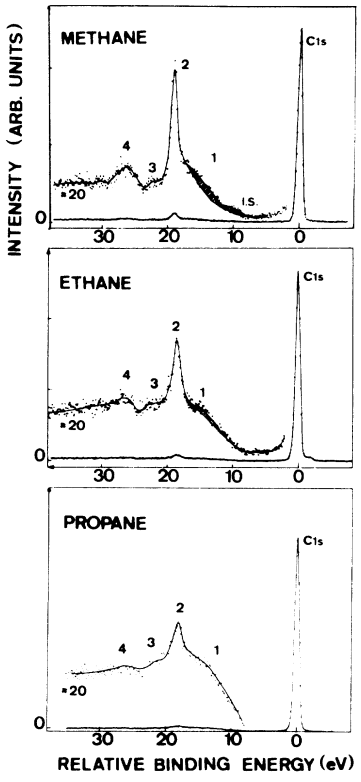

FIG. 7. Shakeup spectra of methane, ethane, and propane.

TABLE V. Excitation energies for the C1*s* shake up in methane, ethane, and propane (eV).

Molecule \ Peak	I.S.	1	2	3	4
methane	9.9	~15	19.23	22.7	26.5
ethane	•••	14.7	18.48	22.5	26.5
propane	•••	~15	17.9	21.5	26.3

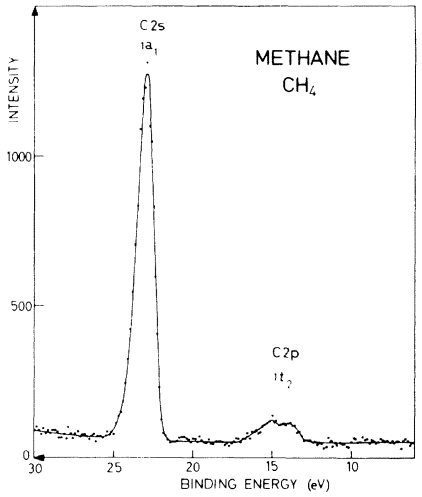

FIG. 8. Valence-electron spectrum of methane.

those obtained earlier for a π-electron system like benzene.[23] Almost identical relaxation energies are obtained (15.9 and 16.2 eV, respectively), but they are caused by different ΔV_A terms (4.68 and 4.02 eV, respectively).

The group-shift model[21,28] partitions the shift on an atom A into partial shifts related to each group of atoms attached to it:

$$\Delta E_A = \sum \Delta E_{\text{group}} + L. \tag{8}$$

Originally derived from the potential model[1] it can be used in the presence of relaxation. In fact, since the group shifts are determined in a least-squares fit, they will include a group relaxation effect. The groups to be considered for an alkane with n carbon atoms are typically: -H and $-C_mH_{2m}CH_3$, $0 \leq m \leq n-2$.

One obvious application would be to put, e.g., all group shifts for $m \geq 1$ equal and so reproduce all the chemical shifts in a model containing only three parameters. However, in this work, we will use our known experimental shifts and solve the corresponding sets of equations for the $-C_mH_{2m}CH_3$ group shifts. In this way we may study the relaxation dependence of the group size. The group shift for -H was taken to be 0.01 eV,[28] thereby defining the reference-level parameter L. In Fig. 6 the calculated $-C_mH_{2m}CH_3$ group shift is plotted as a function of m. As can be seen the group shift is practically constant for $m \geq 3$. In consequence, a model as discussed above, using only three parameters, is justified. The approximate value of -0.3 eV for the $-CH_2C$ group shift obtained from Fig. 6 is in disagreement with an earlier result of -0.06 eV.[28] However, this latter value was determined from one single chemical-shift value only.

In order to estimate to what extent the CNDO approximation affects the results discussed above we performed *ab initio* calculations on methane, ethane, propane, and n-butane. Table III shows that the Koopmans orbital energies, using an extended basis set (STO-4.31G), are practically constant for these molecules, and are increasing rather than decreasing. This trend is also found in the minimal-basis-set calculations (Table IV, column 3). As a further step of refinement *ab initio* ΔSCF (self-consistent field) energies were calculated using the equivalent-core approximation, i.e., the shifts relative to methane were deduced from the thermodynamic model[29] applied to the "reaction":

$$C_2H_6 + NH_4^+ \rightarrow H_3N^+CH_3 + CH_4.$$

Because of limited computer resources, these calculations were performed only with the minimal basis set. The chemical shifts obtained from the ΔSCF calculations are seen to reproduce the decreasing behavior of the experimental shifts. However, as was found for the TPM calculations on the CNDO/2 level, the shifts are overestimated by approximately a factor of 2. This indicates that the nonunit slope (0.50) in Fig. 3 for the correlation of experimental versus TPM chemical shifts is due to the limitations of a minimal-basis de-

TABLE VI. Experimental and calculated binding energies for the valence-electron lines of methane (in eV).

	Experimental results					Theoretical results		
		Hamrin	Banna	Potts	Price[b]	This work		
Line	This work energy[a]	(Ref. 2) Al $K\alpha$	(Ref. 42) Y $M\zeta$	(Ref. 6) He II	(Ref. 4) He II	*Ab initio*[c] STO-4.31G	Ext. Hückel	Mayer[d] (Ref. 25)
1	22.93	23.1	23.05	22.91	23.02	25.66	24.68	23.38
2	14.45	13.6	14.5	14.35	14.4	14.75	15.39	14.29

[a] Computer-fitted value.
[b] Measured on published spectra.
[c] Total energy: $-40.139\,34$ a.u.
[d] Total energy: $-40.472\,32$ a.u. (CI calculation).

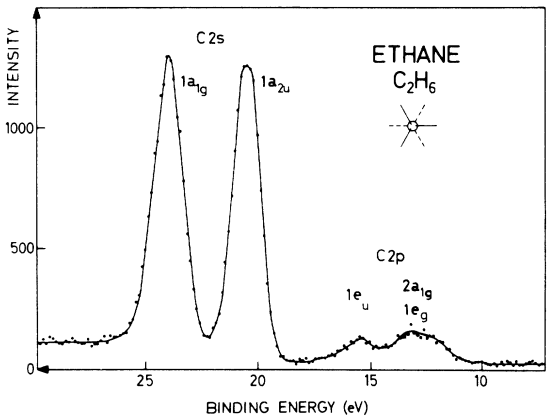

FIG. 9. Valence-electron spectrum of ethane.

scription rather than to the approximations behind the transition-potential model.

C. Shakeup spectra

To complete the study of the core levels we have recorded the shakeup[1] spectra of methane, ethane, and propane (Fig. 7). All the spectra exhibit broad structures at about 15, 22, and 26 eV and a more narrow line at about 19 eV from the main line. One observes a systematic variation in the series. The intensity and the shakeup energy of the latter line is decreasing when the number of carbon atoms is increasing (see Table V).

Each spectrum was also recorded at a lower pressure in order to check the inelastic scattering contribution, which is estimated by the shadowed parts of Fig. 7. The small structure (marked I.S.) in the methane spectrum at 9.9 eV relative to the main line is in good agreement with the $1t_2$-$3s$ and $1t_2$-$4s$ excitations to Rydberg orbitals observed in the electron-impact spectrum reported by Harshbarger *et al.*[30]

The assignment of shakeup spectra from molecules is a rather complex multiplet problem.[31-33] It involves the interaction of the two doublets that can be formed out of the three open shells taking part in the excitation process.[1] From the results of Faegri and Manne[34] it is reasonable to assume that lines 2 and 3 in the methane spectrum originate from shakeup transitions of the type $1t_2$-$2t_2$ and $1t_2$-$3t_2$, respectively. The $1t_2$-nt_2 shakeoff continuum is then likely to start under peak 4. Line 1 might be due to a $1a_1$-na_1 shakeup process. (In this notation, $1a_1$ refers to the valence C $2s$ level; see Fig. 8.) Following the arguments in Refs. 33 and 35 this assignment is also supported by the large width of line 1. The $1a_1$ orbital is strongly C-H bonding and consequently a $1a_1$-na_1 excitation should involve a substantial vibration or dissociation broadening of the corresponding shakeup line.

From the resemblance and the systematic variation between the three recordings of Fig. 7 we then conclude that structures 1 and 2 in the ethane and propane spectra involve transitions from orbitals of C $2s$ and C $2p$ character, respectively. It can be noted that the measurements presented here are quite structureless when compared to the shakeup spectra of, e.g., ethene and acetylene.[36,37] This can be explained by vibrational and dissociative broadening. The effect corresponds to the fact that the optical absorption spectrum of C_2H_6 is continuous while several discrete optical absorption bands are reported for C_2H_4 and C_2H_2.[38]

IV. VALENCE LEVELS

Valence-electron spectra from the first five molecules in the alkane series are shown in Figs. 8–12. The valence-electron lines are numbered from the left ot the right in the spectra, and their binding energies are given in Tables VI–X. When not explicitly indicated within parentheses, the estimated uncertainty of the experimental values is less than 0.03 eV. The tables also list a se-

TABLE VII. Experimental and calculated binding energies for the valence-electron lines of ethane (in eV).

	Experimental results				Theoretical results		
		Hamrin	Potts	Price[b]	This work		
Line	This work energy[a]	(Ref. 2) Al $K\alpha$	(Ref. 6) He II	(Ref. 4) He II	*Ab initio*[c] STO-4.31G	Ext. Hückel	Buenker[d] (Ref. 44)
1	23.91	23.9	23.9	24.17	27.66	26.53	27.56
2	20.42	20.3	20.42	20.48	22.74	21.71	22.68
3	15.35	14.7		15.28	16.24	16.06	16.13
4	12.69	10.7		12.53–13.52	13.48–13.16	14.54–14.17	13.30–12.96

[a] Computer-fitted value.
[b] Measured on published spectra.
[c] Total energy: −79.113 69 a.u.
[d] Total energy: −79.182 26 a.u. (CI calculation).

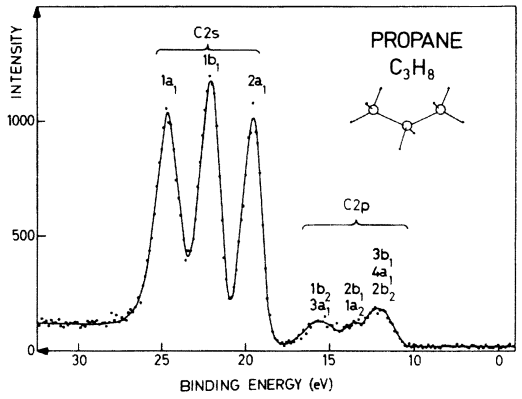

FIG. 10. Valence-electron spectrum of propane.

lection of binding-energy data, determined from x-ray (Al $K\alpha$, Y $M\zeta$) and uv (He II) excited spectra. To interprete the spectra *ab initio* calculations were performed using an STO-4.31G basis set for all molecules except for *n*-pentane, where an STO-3G basis set was used.[39] The results of the calculations are given in the second part of Tables VI–X.

All the alkane valence-electron spectra in Figs. 8–10 show distinct C 2*s* and C 2*p* regions separated by a pronounced energy gap. In contrast to the core-level spectra the valence-orbital regions show little shakeup structure. It should be mentioned that this is not the case for π-electron systems like ethene,[36(a),36(b)] the chloroethenes,[36(a)] and acetylene.[37]

A. Methane (Fig. 8, Table VI)

The molecular orbitals of methane have previously been studied by x-ray and uv excited electron spectroscopy[40] and by theoretical calculations.[41]

The two lines in Fig. 8 correspond to the $1a_1$ (C 2*s* and H 1*s* character) and $1t_2$ (C 2*p* and H 1*s* character) orbitals. They are populated by two and six electrons, respectively. The intensity ratio in the spectrum is 7.24/1, resulting from the large difference in the photoionization cross section for C 2*s* and C 2*p* atomic orbitals. Although the electron line corresponding to the $1t_2$ orbital has a very low intensity, a splitting is clearly observed for this degenerate level. This is also seen in uv and Y $M\zeta$ excited electron spectra, and is explained by the Jahn-Teller effect.[43] The final state of the $1t_2$ photoionization process has a lower symmetry than the ground state of the molecule. Therefore, the degeneracy of the $1t_2{}^2T_2$ ionic state is removed by proceeding to an ionic state of either C_{2v}, D_{2d}, or C_{3v} symmetry.

B. Ethane (Fig. 9, Table VII)

According to extensive *ab initio* calculations[44] the five outermost orbitals in ethane are ordered:

$$(1a_{1g})^2(1a_{2u})^2(1e_u)^4(2a_{1g})^2(1e_g)^4.$$

Four peaks can easily be distinguished in Fig. 9. The two intense lines at 23.91 eV ($1a_{1g}$) and 20.42 eV ($1a_{2u}$) are of C-C bonding and antibonding C 2*s* character, respectively. The full width at half-maximum (FWHM) is 1.64 eV for the $1a_{1g}$ line and 1.46 eV for the $1a_{1u}$ line, which is broader than the $1a_1$ level in methane, 1.30 eV. Vibrational and dissociative broadening are responsible for these large linewidths. In methane the C-H vibrations are important, whereas in ethane also the C-C stretching frequencies contribute to the line profile.

The remaining structures in Fig. 9 are the well-separated peak at 15.35 eV corresponding to the

TABLE VIII. Experimental and calculated binding energies for the valence-electron lines of propane (in eV).

	Experimental results				Theoretical results		
		Potts	Price[b]	Steichen	This work		
Line	This work energy[a]	(Ref. 6) He II	(Ref. 4) He II	(Ref. 48) He II	*Ab initio*[c] STO-4.31G	Ext. Hückel	Murrel (Ref. 49)
1	24.60	24.5	24.55	24.3	28.75	27.59	27.55
2	22.08	22.1	22.16	22.2	25.25	23.78	24.49
3	19.57	19.15	19.59	19.39	21.84	20.42	21.38
4	15.64		15.48		17.01–16.26	16.47–15.91	17.01–15.99
5	13.70		13.76		14.97–14.42	15.22–15.08	14.67–14.32
6	12.04		12.00		12.87–12.82–12.61	14.20–13.96–13.57	12.69–12.37–11.83

[a] Computer-fitted value.
[b] Measured on published spectra.
[c] Total energy: −118.093 55 a.u.

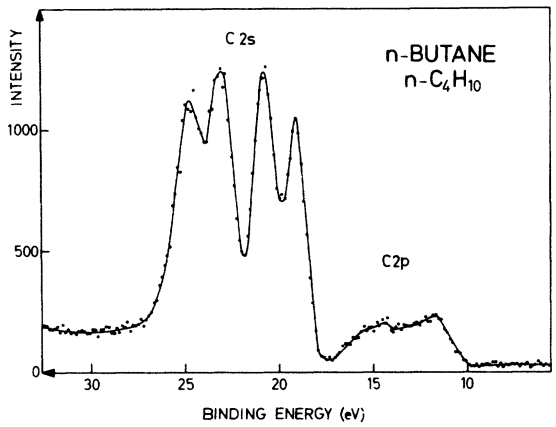

FIG. 11. Valence-electron spectrum of n-butane.

$1e_u$ electron level and the peak at 12.7 eV, which seems to be split in two structures at approximately 13.3 and 12.3 eV. This splitting is in good agreement with data from uv excited electron spectra.[3,4,45] This structure involves the $2a_{1g}$ and the $1e_g$ molecular orbitals but their assignment is still an open question. Moreover, the Jahn-Teller effect should split the $1e_g$ orbital into two components,[3] which makes the orbital assignment rather complicated. This problem has recently been reviewed[46] and the ordering given above seems to be the one agreed upon by most authors.[47]

C. Propane (Fig. 10, Table VIII)

The valence electrons in propane are distributed over ten molecular orbitals. In the spectrum of Fig. 10, however, only six structures can be resolved. The innermost three orbitals of C2s character are easily assigned to the $1a_1$, $1b_1$, and $2a_1$ orbitals at 24.60, 22.08, and 19.57 eV binding energy, respectively. Their corresponding FWHM are 1.86, 1.57, and 1.46 eV. These differences in FWHM are explained by the vibrational broadening of the electron lines.

The C2p region presents only three resolved structures. It is still possible to assign symmetries to these peaks. Indeed, according to the *ab initio* calculations and uv excited electron spectra,[5,47(d)] the binding energies of these molecular orbitals fall into three groups.

D. n-butane (Fig. 11, Table IX)

In the inner valence region in Fig. 11, four distinct structures are found, and are due to the corresponding orbitals of C2s character. Theoretical calculations predict nine orbitals in the C2p region. Only two broad structures appear in the recorded spectrum. The experimental valence-electron binding energies from methane to n-butane are plotted versus the *ab initio* STO-4.31G results in Fig. 13. The correlation is satisfying, which indicates an overall consistency of the assignments.

E. n-pentane (Fig. 12, Table X) and n-nonane (Fig. 14)

For $n \geq 5$ even the C2s orbitals become unresolved. Only three peaks can clearly be seen in the C2s region of n-pentane (Fig. 12). The electron lines corresponding to the five molecular orbitals are vibrationally broadened and overlap in energy. In the C2p region as many as 11 orbitals are theoretically expected. It is not any more possible to resolve by computer fitting the structure between 10- and 15-eV binding energy. Therefore no assignment of the molecular orbitals is attempted. Also for n-nonane the C2p region is completely smeared out. In the C2s region nine orbitals are

TABLE IX. Experimental and calculated binding energies for the valence-electron lines of n-butane (in eV).

	Experimental results				Theoretical results	
		Potts	Price[b]	Steichen	This work	
Line	This work energy[a]	(Ref. 6) He II	(Ref. 4) He II	(Ref. 48) He II	*Ab initio*[c] STO-4.31G	Ext. Hückel
1	24.73(5)	24.7	24.63	24.60	29.06	27.90
2	23.00(5)	23.0	22.99	23.00	26.63	25.28
3	20.81	20.7	20.74	20.70	23.37	22.01
4	19.11	18.80	18.98	18.94	21.53	20.15
5	15.0		15.72		17.17	16.58
6			14.46		15.91–15.52–15.35	15.69–15.62–15.42
7	12.1		12.67		13.96–13.32	14.59–14.52
8			11.36		12.78–12.30–12.22	14.23–13.87–13.23

[a] Computer-fitted value.
[b] Measured on published spectra.
[c] Total energy: −157.068 80 a.u.

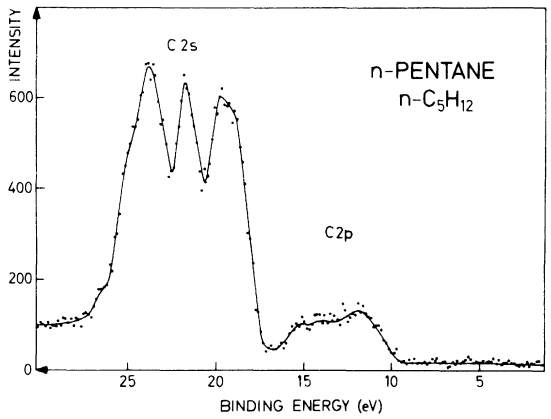

FIG. 12. Valence-electron spectrum of n-pentane.

theoretically located, but only five structures are resolved in the spectrum. The lines are now so densely packed that the spectrum starts to resemble a band structure, rather than a collection of distinct lines.

F. Formation of a band structure

The linear alkanes have been extensively studied by different theoretical methods.[50] The results are consistent with the *ab initio* STO-3G calculations presented in Fig. 15, which will illustrate our discussions.

For a hydrocarbon of formula C_nH_{2n+2} the valence-electron region contains $6n+2$ electrons distributed among $3n+1$ energy levels. These are divided into two groups, each of which contains $2n+1$ and n molecular orbitals, respectively. The first group, centered around 13–14-eV binding energy, is mainly composed of orbitals of C $2p$ and H1s character, which form the C-H bonds. However, with increasing n this band will also contain a small amount of C2s character. The higher cross section for this atomic symmetry causes a noticeable increase of the C$2p$ band intensity. An energy gap (at least 3 eV) separates this first group of energy levels from the second one, which extends from ~20- to ~29-eV binding energy. The molecular orbitals in the latter group are mainly composed of C-C bonding and antibonding combinations of C2s atomic orbitals. The number of levels in the C2s region is equal to the number of carbon atoms in the alkane chain. The $1a_1$ level in methane splits into two levels in ethane, three levels in propane, etc. Since the energy levels are spread out over a limited energy range of a few electron volts the spacing between each level decreases with an increasing number of carbon atoms. For large n this leads to the formation of a band structure. As can be seen in Fig. 15 the increase of the theoretical C2s bandwidth is small for $n \geq 6$.

Figure 16 illustrates schematically the buildup of a band structure, as it is recorded on the alkanes valence-band spectra. These molecules can be considered as progressive steps in the formation of a quasilinear one-dimensional infinite solid, polyethylene. From the successive valence bands one can also observe when the ESCA spectrum of a finite linear molecule will be indistinguishable from that of polyethylene. This tells us how large the system must be to approximate the band structure of an infinite solid. Already for n-tridecane ($n = 13$) no fine substructure can be resolved, as was still the case for n-nonane. Moreover, from Fig. 17, it is obvious that this valence band of gaseous n-$C_{13}H_{28}$ is very similar to the solid-phase spectrum of n-$C_{36}H_{74}$ (hexatriacontane). The only difference is the high background in the solid spectrum on the low-kinetic-energy side of the lines. This is explained by inelastic scattering of the outgoing photoelectrons. As has previously been shown,[51] the n-$C_{36}H_{74}$ spectrum is essentially the same as that of polyethylene. We conclude that 13

TABLE X. Experimental and calculated binding energies for the inner-valence-electron lines of n-pentane (in eV).

	Experimental results				Theoretical results	
		Potts	Price[b]	Steichen	This work	
Line	This work energy[a]	(Ref. 6) He II	(Ref. 4) He II	(Ref. 48) He II	*Ab initio*[c] STO-3G	Ext. Hückel
1	25.0(2)	24.8	24.72	24.7	28.22	28.20
2	23.6(1)	23.7	23.96	24.00	26.35	26.47
3	21.79	21.7	22.08	21.10	23.63	23.42
4	19.87(5)	19.9	20.05	19.76	20.88	20.88
5	18.70(5)	18.74	18.89	18.68	20.19	19.95

[a] Computer-fitted value.
[b] Measured on published spectra.
[c] Total energy: −194.034 01 a.u.

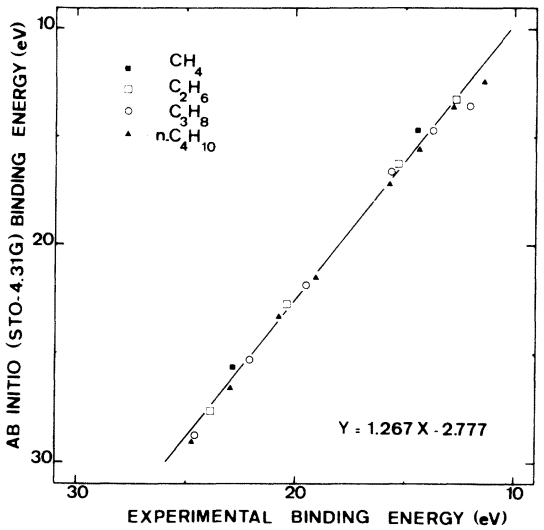

FIG. 13. Correlation diagram of the alkane molecular energy levels: *ab initio* calculated values versus experimental ESCA data.

atoms in the chain are certainly sufficient to approximate an infinite solid. An addition of more carbon atoms will not affect the spectrum significantly.

V. CONCLUSIONS

The alkanes have been shown to provide a convenient series for the study of the influence of the molecular size on the electron relaxation energy. The binding energy was found to be monotonically decreasing with an increasing number of carbon atoms, whereas simple electronegativity arguments and the ground-state potential model predict the opposite trend. Including relaxation by means of the transition-potential model gives a more satisfactory description of the orbital energies. The analysis of the TPM populations indicates that the screening of the core hole is practically constant; i.e., the electron flow onto the ionized atom always amounts to 1.0 electron. Consequently, the potential set up by the redistributed charge on the other atoms rules the variation of the relaxation energy. The effective screening radius increases with the size of the molecule and reaches an asymptotic value of only 1.7 Å. It is also found that the molecular size-effect on the group relaxation is fully developed already for the $-C_3H_6$ group.

Systematic changes in the shakeup spectra of methane, ethane, and propane were observed. The most prominent peak in these spectra was tentatively assigned to a transition from a C2*p*-H1*s* bonding orbital.

Orbital energies from *ab initio* calculations on the first five *n*-alkanes using an extended basis set were found to correlate successfully with the experimental valence-electron binding energies. The molecules of the series were discussed in terms of successive steps in the formation of the valence-

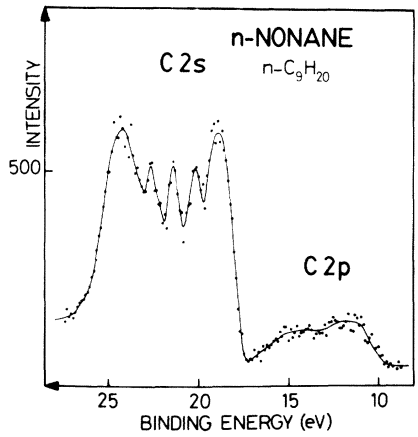

FIG. 14. Valence-electron spectrum of *n*-nonane.

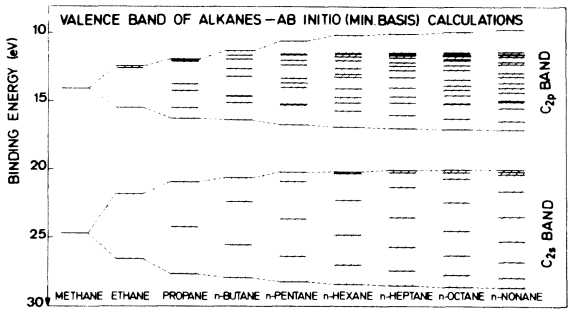

FIG. 15. *Ab initio* analysis (minimal basis, STO-3G) of the molecular orbitals of the alkanes.

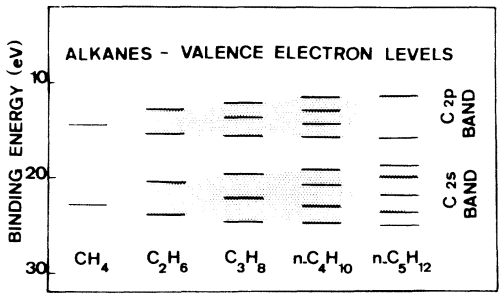

FIG. 16. Diagram of the formation of valence-band structures in the alkanes, as observed by ESCA.

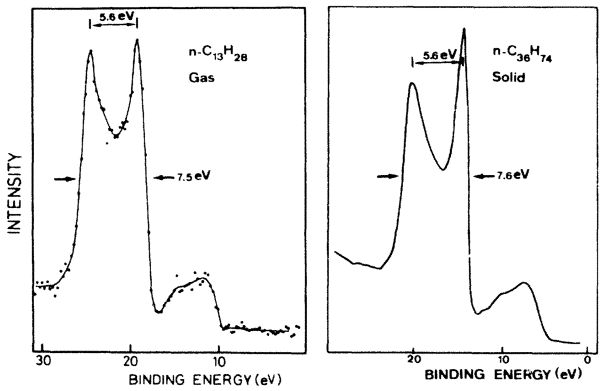

FIG. 17. Valence-electron spectra of n-$C_{13}H_{28}$ and n-$C_{36}H_{74}$ recorded, respectively, in the gas and solid phases. The two spectra are essentially similar.

band structure of the infinite one-dimensional solid polyethylene. We have shown that the essential features in the polyethylene valence-band structure are already present in the n-nonane and n-tridecane valence-electron spectra. The individual orbitals, which still can be partly resolved in the C 2s region of n-nonane are completely smeared out in the spectrum of n-tridecane. In this respect n-tridecane can serve as a finite-system model for the infinite linear polymer.

ACKNOWLEDGMENTS

We are very grateful to Professor J. M. André and Dr. J. Delhalle (Applied Theoretical Chemistry Group, Facultés Universitaires de Namur), who have communicated their *ab initio* analysis of the alkane molecular orbitals, and allowed access to their computer facilities. We would like also to express our gratitude to Dr. O. Goscinski (Quantum Chemistry Group, University of Uppsala) and Dr. R. Manne (Department of Chemistry, University of Bergen) for helpful discussions and communication of results prior to publication. One of the authors (J. J. P.) thanks the Fonds National de la Recherche Scientifique (Belgium) for financial support.

*Facultés Universitaires, Laboratoire de Spectroscopie Electronique 61, Rue de Bruxelles, B-5000, Namur, Belgium.

[1]K. Siegbahn, C. Nordling, G. Johansson, J. Hedman, P. F. Heden, K. Hamrin, U. Gelius, T. Bergmark, L. O. Werme, and Y. Baer, *ESCA Applied to Free Molecules* (North-Holland, Amsterdam, 1969).

[2]K. Hamrin, G. Johansson, U. Gelius, A. Fahlman, C. Nordling, and K. Siegbahn, Chem. Phys. Lett. 1, 613 (1968).

[3]D. W. Turner, C. Baker, A. D. Baker, and C. R. Brundle, *Molecular Photoelectron Spectroscopy* (Wiley, New York, 1970).

[4]W. C. Price, A. W. Potts, and D. G. Streets, in *Electron Spectroscopy*, edited by D. A. Shirley (North-Holland, Amsterdam, 1972), p. 187.

[5]A. W. Potts and W. C. Price, cited in D. F. Brailsford and B. Ford, Mol. Phys. 18, 621 (1970).

[6]A. W. Potts and D. G. Streets, J. Chem. Soc. Faraday Trans. II, 875 (1974).

[7](a) J. M. André, J. Delhalle, S. Delhalle, R. Caudano, J. J. Pireaux, and J. J. Verbist, Chem. Phys. Lett. 23, 206 (1973); (b) J. Delhalle, J. M. André, S. Delhalle, J. J. Pireaux, R. Caudano, and J. J. Verbist, J. Chem. Phys. 60, 595 (1974).

[8]J. J. Pireaux, R. Caudano, J. Riga, and J. J. Verbist (unpublished).

[9]J. J. Pireaux, Ph. D. thesis (Facultés Universitaires de Namur, 1976) (unpublished).

[10]U. Gelius, in *Electron Spectroscopy*, edited by D. A. Shirley (North-Holland, Amsterdam, 1972), p. 311.

[11]U. Gelius, E. Basilier, S. Svensson, T. Bergmark, and K. Siegbahn, J. Electron Spectrosc. 2, 405 (1973).

[12]G. Johansson, J. Hedman, A. Berndtsson, M. Klasson, and R. Nilsson, J. Electron Spectrosc. 2, 295 (1973).

[13]T. D. Thomas, J. Chem. Phys. 52, 1373 (1970).

[14]W. B. Perry and W. L. Jolly, Chem. Phys. Lett. 17, 611 (1972).

[15]D. A. Shirley, Adv. Chem. Phys. 23, 85 (1973).

[16]U. Gelius, S. Svensson, H. Siegbahn, E. Basilier, Å. Faxälv, and K. Siegbahn, Chem. Phys. Lett. 28, 1 (1974).

[17]M. S. Banna and D. A. Shirley, LBL Report 3491, 1975 (unpublished).

[18]W. H. E. Schwarz, J. Electron. Spectrosc. 6, 377 (1975).

[19]K. Siegbahn, C. Nordling, A. Fahlman, R. Nordberg, K. Hamrin, J. Hedman, G. Johansson, T. Bergmark, S-E. Karlsson, I. Lindgren, and B. Lindberg, *ESCA. Atomic, Molecular and Solid State Studied by Means of Electron Spectroscopy* (Almqvist and Wiksells, Uppsala, 1967).

[20]U. Gelius and K. Siegbahn, Trans. Faraday Soc. 54, 2571 (1972).

[21]U. Gelius, Phys. Scr. 9, 133 (1974).

[22]G. Howat and O. Goscinski, Chem. Phys. Lett. 30, 87 (1975).

[23]H. Siegbahn, R. Medeiros, and O. Goscinski, J. Electron Spectrosc. 8, 149 (1976).

[24]O. Goscinski, B. T. Pickup, and G. Purvis, Chem. Phys. Lett. 22, 167 (1973).

[25]W. Meyer, J. Chem. Phys. 58, 1017 (1973).

[26]O. Goscinski, M. Hehenberger, B. Roos, and P. Siegbahn, Chem. Phys. Lett. 33, 427 (1975).

[27]O. Goscinski, G. Howat, and T. Åberg, J. Phys. B 8, 11 (1975).

[28]U. Gelius, P. F. Heden, J. Hedman, B. J. Lindberg, R. Manne, R. Nordberg, C. Nordling, and K. Siegbahn, Phys. Scr. 2, 70 (1970).

[29]W. L. Jolly and D. N. Hendrickson, J. Am. Chem. Soc.

92, 1863 (1970).
[30](a) W. R. Harshbarger, M. B. Robin, and E. N. Lassettre, J. Electron Spectrosc. 1, 319 (1973); (b) W. R. Harshbarger and E. N. Lassettre, J. Chem. Phys. 58, 1505 (1973).
[31](a) M. Wood, Chem. Phys. Lett. 5, 471 (1974); (b) I. H. Hillier and J. Hendrick, University of Manchester Report M13 9PL, 1974 (unpublished); (c) M. F. Guest, I. H. Hillier, V. R. Saunders, and M. H. Wood, Proc. R. Soc. A 333, 201 (1973).
[32]H. Basch, J. Electron Spectrosc. 5, 463 (1974).
[33]S. Svensson, H. Ågren, and U. I. Wahlgren, Chem. Phys. Lett. (to be published).
[34]K. Faegri and R. Manne (unpublished).
[35]U. Gelius, J. Electron Spectrosc. 5, 985 (1974).
[36](a) A. Berndtsson, E. Basilier, U. Gelius, J. Hedman, M. Klasson, R. Nilsson, C. Nordling, and S. Svensson, Phys. Scr. 12, 235 (1975); (b) M. S. Banna and D. A. Shirley, LBL Report 3479, 1975 (unpublished), to be published in J. Electron Spectrosc.
[37]P-Å Malmqvist, E. Basilier, U. Gelius, J. J. Pireaux, S. Svensson, and K. Siegbahn (unpublished).
[38]G. Herzberg, *Electronic Spectra of Polyatomic Molecules* (Van Nostrand, Princeton, 1966).
[39]In its STO-3G minimal basis version, the *ab initio* program GAUSSIAN 70 approximates each Slater-type orbital by three Gaussian functions. The extended basis STO-4.31G version used four Gaussian inner-shell atomic orbitals and valence orbitals split into three Gaussian inner parts and one Gaussian outer parts. See W. J. Herhe, R. F. Stewart, and J. A. Pople, J. Chem. Phys. 51, 2657 (1969); also Ref. 41.
[40]*Handbook of Spectroscopy*, edited by J. W. Robinson (Chemical Rubber, Cleveland, 1974), Vol. I.
[41]L. Radom and J. A. Pople, M.T.P. Int. Rev. Sci. 71 (1972).
[42]M. S. Banna and D. A. Shirley, LBL Report 3478, 1975 (unpublished).
[43]H. A. Jahn and E. Teller, Proc. R. Soc. A 161, 220 (1937).
[44]R. J. Buenker and S. D. Peyerimhoff, Chem. Phys. 8, 56 (1975).
[45]C. P. Anderson, Ph. D. thesis (University of Tennessee, 1973) (unpublished).
[46]C. Sandorfy, Nato Adv. Study Inst. Ser. Series C8 Chem. Proc. Adv. Study Inst. 1973 (1974), p. 177 (unpublished).
[47](a) A. D. Baker, C. Baker, C. R. Brundle, and D. W. Turner, Int. J. Mass Spectrom. 1, 285 (1968); (b) A. D. Baker, D. Betteridge, N. R. Kemp, and R. E. Kirby, J. Mol. Struct. 8, 75 (1971); (c) J. W. Rabalais and A. Katrib, Mol. Phys. 27, 923 (1974); (d) R. G. Dromey and J. B. Peel, J. Mol. Struct. 23, 53 (1974).
[48]J. Steichen, Ph. D. thesis (Rice University Houston, 1973) (unpublished).
[49]J. N. Murrel and W. Schmidt, J. Chem. Soc. Faraday Trans. II, 1709 (1972).
[50](a) R. Hoffman, J. Chem. Phys. 40, 2047 (1963); (b) Yu. A. Kruglyak, Russ. J. Phys. Chem. 41, 133 (1967); (c) Ts. Lyast and N. P. Poshyunaite, Zh. Strukt. Khim. 2, 496 (1971); (d) A. Deplus, G. Leroy, and D. Peeters, Theor. Chim. Acta 36, 109 (1974); (e) Ph. Degand, G. Leroy, and D. Peeters, Theor. Chim. Acta 30, 243 (1973); (f) P. N. Dyachkov and A. A. Levin, Theor. Chim. Acta 33, 323 (1974); 36, 181 (1975); (g) D. F. Brailsford and B. Ford, Mol. Phys. 18, 621 (1970); (h) W. C. Herndon, Chem. Phys. Lett. 10, 460 (1971); (i) J. M. André, Ph. Degand, and G. Leroy, Bull. Soc. Chim. Belg. 80, 585 (1971).
[51]J. J. Pireaux, R. Caudano, and J. Verbist, in *Electron Spectroscopy. Progress in Research and Applications*, edited by R. Caudano and J. Verbist (Elsevier, Amsterdam, 1974), p. 267.

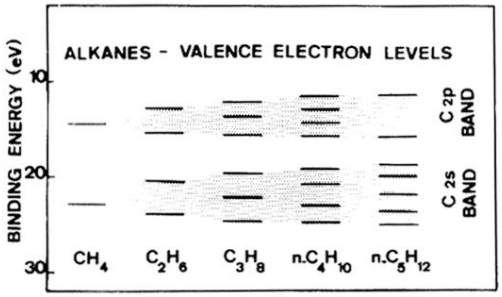

FIG. 16. Diagram of the formation of valence-band structures in the alkanes, as observed by ESCA.